Structural Analysis of Silanediols as Transition-State-Analogue Inhibitors of the Benchmark Metalloprotease Thermolysin†,‡

Douglas H. Juers,*,§,|| Jaeseung Kim,⊥,# Brian W. Matthews,*,|| and Scott McN. Sieburth*,#,¶

Institute of Molecular Biology, Howard Hughes Medical Institute and Department of Physics, University of Oregon, Eugene, Oregon 97403, Department of Chemistry, State University of New York at Stony Brook, Stony Brook, New York 11794-3400, and Department of Chemistry, Temple University, Philadelphia, Pennsylvania 19122

Received July 12, 2005; Revised Manuscript Received October 24, 2005

ABSTRACT: Dialkylsilanediols have been found to be an effective functional group for the design of active-site-directed protease inhibitors, including aspartic (HIV protease) and metallo (ACE and thermolysin) proteases. The use of silanediols is predicated on its resemblance to the hydrated carbonyl transition-state structure of amide hydrolysis. This concept has been tested by replacing the presumed tetrahedral carbon of a thermolysin substrate with a silanediol group, resulting in an inhibitor with an inhibition constant $K_i = 40$ nM. The structure of the silanediol bound to the active site of thermolysin was found to have a conformation very similar to that of a corresponding phosphonamidate inhibitor ($K_i = 10$ nM). In both cases, a single oxygen is within bonding distance to the active-site zinc ion, mimicking the presumed tetrahedral transition state. There are binding differences that appear to be related to the presence or absence of protons on the oxygens attached to the silicon or phosphorus. This is the first crystal structure of an organosilane bound to the active site of a protease.

The design of metalloprotease inhibitors for adaption as new pharmaceuticals has become commonplace (*1*−*5*). Structurally novel enzyme inhibitors have also led to a deeper understanding of enzymatic action and ligand−receptor interaction (*4*, *5*). Inhibitors of the metalloprotease angiotensin-converting enzyme were the first protease inhibitors to become commercially successful drugs (*6*), and many other metalloproteases are potential or actual pharmaceutical targets (*7*, *8*).

Thermolysin was one of the first metalloproteases to have its structure solved crystallographically (*9*), revealing an active-site zinc ion that activates the scissile amide bond (**1**, Figure 1) toward the attack by water **(2**), and stabilizes the resulting tetrahedral intermediate (*10*). At the center of the metalloprotease inhibitor design is selection of a functional group that will interact with the metal. Thiols **4** have an intrinsic affinity for zinc and have been commonly deployed in this capacity (*4*, *5*, *11*). Ketones (hydrated as in **5**) have been found to be useful metalloprotease inhibitors (*12*), and the strong chelation of zinc by hydroxamic acids **6** has given rise to potent inhibitors (*13*). Anionic groups, such as carboxylates **7** and phosphinates **8**, in which the charge provides a Coulombic attraction to the zinc cation, are found in many successful inhibitors (*4*, *5*). Silanediols **9** are recently introduced mimics of the unstable hydrated carbonyl **2**, employing a central silicon atom, the element most similar to carbon.

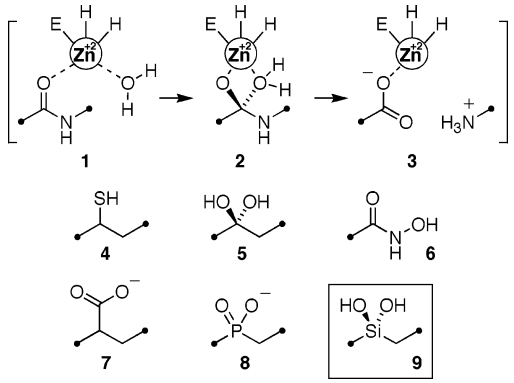

FIGURE 1: Hydrolysis of peptides catalyzed by the active-site zinc and zinc-binding groups used to design synthetic metalloprotease inhibitors.

Silanediol-based protease inhibitors have been prepared by substitution of the silanediol into a known inhibitor in three instances: replacing the alcohol in **10b** to give an HIV protease inhibitor **10a** (Figure 2) (*14*), replacing a ketone in **11b** to inhibit angiotensin-converting enzyme with **11a** (*15*−*17*), and replacing a phosphinic acid in **12b** for inhibition of thermolysin with **12a** (*18*, *19*). Thermolysin inhibitors **12a**−**d** employ the second row elements silicon and phosphorus, which are of similar size, to create the zinc-binding moiety. For the silanediol **12a**, the oxygen (Y) of phosphorus acids

† This work was supported in part by grants from the NIH to B. W. M. (GM20066) and S. McN. S. (HL62390).

‡ The coordinates and structure factors have been deposited in the Protein Data Bank under code 1Y3G.

* To whom correspondence should be addressed. Telephone: (509) 527-5229. Fax: (509) 527-5904. E-mail: juersdh@whitman.edu (D.H.J.); Telephone: (215) 204-7916. Fax: (215) 204-1532. E-mail: scott.sieburth@temple.edu (S.McN.S.); Telephone: (541) 346-2572. Fax: (541) 346-5870. E-mail: brian@uoxray.uoregon.edu (B.W.M.).

§ Current address: Department of Physics, Whitman College, Walla Walla, Washington 99362.

|| University of Oregon.

⊥ Current address: Institut Pasteur Korea, Division of Chemistry, 39-1 Hawolgok-dong Seongbuk-gu, Seoul, 136-791 Korea.

State University of New York at Stony Brook.

¶ Temple University.

10.1021/bi051346v CCC: $30.25
Published on Web 11/24/2005

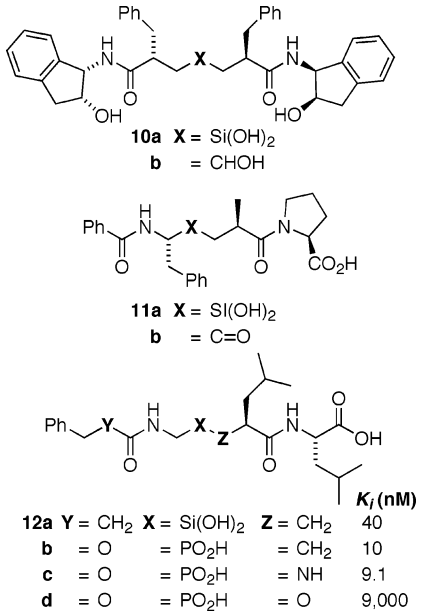

FIGURE 2: Silanediol protease inhibitors and their carbon and phosphorus analogues with inhibition constants (*18*, *19*).

12b−**d** was replaced with a methylene group, a consequence of the strongly acidic conditions used to prepare the silanediol (*20*). The replacement of a Cbz (benzyloxycarbonyl) group (Y = O, **12b**−**d**) with a dihydrocinnamoyl group (Y = CH_2, **12a**) was expected to be of little consequence, because that oxygen has no significant interaction with the enzyme.

While the advantages of using a phosphorus anion (**12b**−**d**, at pH > 4) for the interaction with the active-site zinc cation are obvious, the use of these phosphorus groups as pharmaceutical agents requires their delivery in the form of an uncharged ester prodrug that must be hydrolyzed *in vivo* (*21*). The neutrality of a silanediol group could allow its use without protection or activation.

Silanediols **11a** and **12a** are both low nanomolar inhibitors of metalloproteases, yet dialkylsilanediols are not well-known for their abilities to bind metals. A cyclic siloxane surrounding a potassium ion has been reported (*22*), and structures of zinc ions chelated by silicates have been published (*23*). Trialkylsilanols have also been promoted as transition-metal ligands (*24*, *25*).

To more fully investigate how a silanediol group interacts with the active site of a metalloprotease, the silanediol **12a** was crystallized with thermolysin. Phosphinic acid **12b** has been discussed by Bartlett et al. (*26*) and Grobelsky et al. (*27*). Here, we describe the crystal structure of the silanediol **12a** bound to thermolysin and compare this to complexes between the thermolysin and phosphonamidate **12c** [PDB ID 5TMN (*28*)] and phosphonate **12d** [PDB ID 6TMN (*29*)].

EXPERIMENTAL PROCEDURES

Inhibitor/Enzyme Preparation and Crystallization. The silanediol was prepared as previously reported (*19*). Thermolysin from *Bacillus thermoproteolyticus* was purchased from Calbiochem and stored at −20 °C. Hexagonal crystals (space group, $P6_122$) were grown using vapor diffusion with sitting drops based on the procedure described by Hausrath et al. (*30*). Briefly, the protein was dissolved at 100 mg/mL in 50 mM MES at pH 6.0 and 45% (v/v) DMSO (dimethyl sulfoxide). With a well solution of 30% (w/v) ammonium sulfate, sitting drops of 10 μL of protein and 10 μL of buffer (50 mM MES at pH 6.0, 45% (v/v) DMSO, and 1.0 M NaCl) were then prepared. After the crystals grew for several days, they were transferred in one step to a solution of 25 mM MES at pH 6.0, 500 mM NaCl, 1 mM $CaCl_2$, and 5% (v/v) DMSO. The crystals were then soaked for 3 days in the above buffer with 50 μM silanediol added.

Table 1: Data Collection and Refinement Statistics

data collection statistics[a]	
space group, $P6_122$;	
cell dimensions, $a = b = 93.52$ Å, $c = 131.77$ Å	
resolution range, 31.9−2.1 Å	
completeness, 96.1% (93.1%)	
R_{merge},[b] 11.1% (34.0%)	
$I/\sigma(I)$, 6.4 (2.2)	
redundancy, 6.0 (6.2)	
refinement statistics	
resolution range, 31.9−2.1 Å	
number of reflections,	
18 553 (working set)/1015 (test set)	
R factor,[c] 15.5% (working set)/15.8% (all data);	
R_{free}, 22.5%	
rms deviations	
bond lengths, 0.008 Å	
bond angles, 1.1°	
B factor correlations, 4.9 Å^2	
mean B factors	
protein atoms (main chain), 19 Å^2	
protein atoms (side chain), 26 Å^2	
inhibitor atoms,[d] 17 (32) Å^2	
solvent atoms, 33 Å^2	

[a] Values in parentheses refer to the high-resolution bin (2.15−2.10 Å). [b] R_{merge} gives the agreement between symmetry-related reflections. $R = \sum_{hkl}\sum_i|I_i(hkl)\sum\langle I(hkl)\rangle|/\sum_{hkl}\sum_i I_i(hkl)$. [c] Working set = the 18 553 reflections used for refinement. R_{free} = R factor based on the 1015 reflections not used for refinement. [d] The benzyl group of the inhibitor is disordered. When this group is excluded, the mean inhibitor B factor is 17 Å^2. Including it, the mean inhibitor B factor is 32 Å^2.

Crystallography. After the crystal with bound ligand was mounted in a glass capillary tube, diffraction data were collected using a Rigaku rotating anode X-ray source and R-Axis IV image plate detector. A total of 50 images were recorded, each with an exposure time of 15 min during a 1.0° oscillation. The images were processed with Mosflm (*31*), and the data were reduced with Scala (*32*). Refinement was carried out with TNT (*33*) against a working set of 18 553 reflections, with a random test set of 1015 reflections (or about 5%) excluded from the refinement process for cross-validation (*34*). Using a native thermolysin structure (PDB ID 8TLN) as a starting model, an initial $F_o^{silanediol} - F_o^{native}$ electron-density map was ambiguous, in part because of the presence of a dipeptide in the active site in the native structure (*35*). For refinement, to decouple the test set and working set, all solvent molecules and ligand atoms were removed from the starting model, the B factors were set to the Wilson B factor (16.4) and a random coordinate shift was applied to all atoms such that the rms shift was 1.0 Å (*33*, *34*). Some refinement was then done using rigid-body refinement of the whole molecule followed by individual atom positional refinement using conjugate direction minimization of a least-squares target function (*33*). The binding mode for the silanediol could then be discerned from a $F_o^{silanediol} - F_c^{omit}$ electron-density map. The ligand was built into this map; solvent molecules were added; and the structure was further refined with several rounds of map

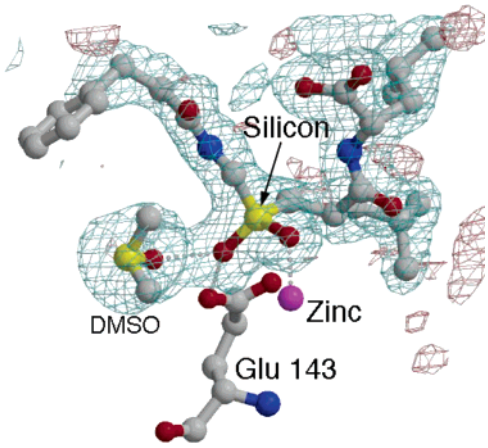

FIGURE 3: Refined model of the silanediol **12a** in the active site of thermolysin. The electron density shown is $F_o^{silanediol} - F_c^{omit}$, where F_c^{omit} are structure factors based on a model refined with no atoms in the active site. The phases were also calculated from this omit structure. The density is contoured at $+3\sigma$ (blue) and -3σ (red). For more detail on the binding interactions, see Figure 4. The figure was prepared with MOLSCRIPT (*36*) and Raster3D (*37*).

inspection with manual side-chain, ligand, and water adjustment followed by atomic coordinate and *B*-factor refinement by minimization. Data collection and refinement statistics are given in Table 1. Coordinates and structure factors have been deposited in the Protein Data Bank (PDB ID 1Y3G).

RESULTS AND DISCUSSION

The structure of the thermolysin/silanediol complex is well-refined with acceptable geometry and excellent agreement with the diffraction data (Table 1). The silanediol inhibitor **12a** binds with the tetrahedral silicon center mimicking the proposed transition state for peptide hydrolysis, with the zinc ion interacting with both silicon hydroxyls (Figures 2 and 3). Glu 143, which is thought to help activate the attacking water molecule, interacts preferentially with one of the silicon oxygens (Figure 3). Additionally, a DMSO molecule is seen binding next to and interacting with the inhibitor.

Overall, the silanediol inhibitor **12a** binds similarly to the phosphonamidate **12c** and phosphonate **12d** (Figure 4). There are some differences, which increase as one moves along the inhibitor from its C-terminal leucine to its N-terminal Cbz group. The C-terminal residues are positioned essentially the same relative to the enzyme. The silane group is shifted somewhat from the phosphate group, and the N-terminal benzyl group is repositioned substantially.

There are three principal binding differences, and these can be rationalized on the basis of the structural differences between the inhibitors (Table 2 and Figure 4). Phosphorus and silicon have slightly different covalent radii (1.06 Å for phosphorus and 1.11 Å for silicon), as well as differences in their intrinsic bond angles (*38*). With the silanediol

Table 2: Polar Interaction Distances (Å) between the Enzyme and Inhibitor for the Silanediol **12a** and Phosphonamidate **12c**[a]

inhibitor atom[b]	contacting atom (protein or bound solvent/ion) and distance (Å)				difference (Å)
	silanediol (1Y3G)		zgpll (5TMN)		
I1 O	Wat 606 O	**2.8**	same	**2.6**	−0.2
I2 N	Ala 113 O	**2.9**	Wat 362 O	**2.9**	0.0
I2 O1	Glu 166 OE1	**3.1**	same	3.1	0.0
	His 231 NE2	**2.6**	same	**2.9**	0.3
	Zn++	1.9	same	2.1	0.2
I2 O2	DMSO 802 O	**2.6**	Wat 362 O	**2.7**	0.1
I3 CH2 (N)	Ala 113 O	3.0	same	**3.0**	0.0
I3 O	Arg 203 NH1	**2.9**	same	**3.0**	0.1
	Arg 203 NH2	**2.9**	same	**3.0**	0.1
I4 O	Asn 112 ND2	**2.9**	same	**3.0**	0.1
	Wat 606 O	**2.5**	same	**2.6**	0.1
I4 OXT	Wat 553 O	**2.7**	same	**2.8**	0.1
	Wat 604 O	**2.5**	same	**2.6**	0.1

[a] The contact distances between the hydrogen donor and acceptor for all potential hydrogen bonds made by the silanediol or the phosphonamidate inhibitor to the enzyme or solvent are listed. Hydrogen bonds were determined with HBPLUS (*44*) using a 3.2 Å donor−acceptor cutoff from the coordinates for the complexes between the thermolysin and silanediol (PDB ID 1Y3G) and the thermolysin and phosphonamidate (PDB ID 5TMN). Non-hydrogen-bonding interaction distances were calculated with EdPDB (*45*). Bold interaction distances indicate that the contact satisfies HBPLUS hydrogen-bonding requirements. Regular-type interaction distances indicate that the contact does not satisfy hydrogen-bonding requirements, either because of incorrect angles or incompatible donor and acceptor. We show these regular-type distances for comparison purposes. [b] Inhibitor atoms are listed by the inhibitor residue number (e.g., I1−I4, corresponding to Figure 4) and atom name. In most cases, the inhibitors contact the same atoms in both structures.

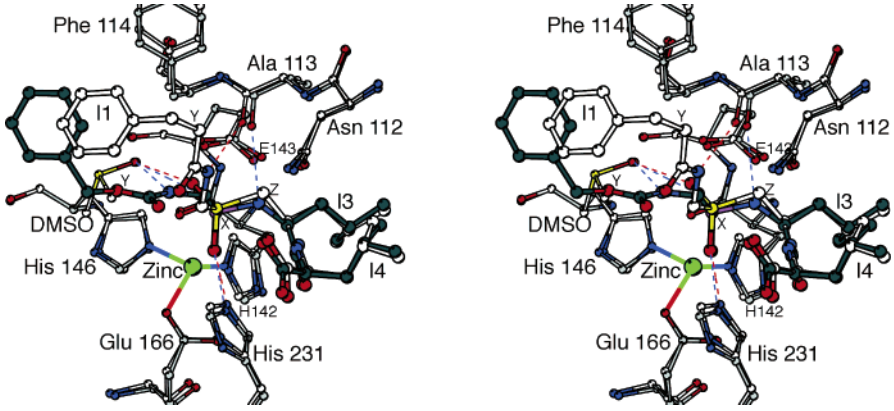

FIGURE 4: Wall-eyed stereoview showing the binding detail, comparing the silanediol **12a** (white carbons) to the phosphonamidate **12c** (gray carbons). The amino acids or amino acid analogues comprising the inhibitors are labeled I1−I4. The atoms labeled X, Y, and Z are identical to those in Figure 2. Some key potential hydrogen bonds that are discussed in the text are indicated with dashed lines. The phosphonate **12d** (not shown) binds essentially identically to the phosphonamidate **12c** (maximum difference of 0.2 Å) (*29*). The figure was prepared with MOLSCRIPT (*36*).

inhibitor **12a**, the silicon atom has hydroxyl substituents, while the phosphorus of the phosphonamidate **12c** has oxyanion substituents. This accounts for two of the observed differences. First, His 231 shifts about 0.3 Å closer to one of the silicon hydroxyls compared to its distance from the equivalent phosphorus oxygen (Table 2). Histidine 231 is considered to make a critical interaction between the enzyme and the hydrated transition state (*39*, *40*), and the close interaction with the silicon hydroxyl reflects the outstanding hydrogen bonding associated with silanols (*41*, *42*). Second, a DMSO molecule has a close interaction (2.6 Å) between its oxygen and the other hydroxyl of the silanediol (Figure 3), suggesting that the DMSO oxygen, which should have no attached hydrogens, is accepting a hydrogen bond from the silanol. This would not be possible with the phosphonamidate oxygen, and no DMSO was observed at this site in the phosphonamidate complex.

The second structural difference between the inhibitors is that the silanediol **12a** has a carbon (Z, Figure 2) attached to the silicon (X), whereas there is a nitrogen bonded to the phosphorus of the phosphonamidate **12c** and an oxygen in the case of the phosphonate **12d** (Figure 2). This carbon (Z) precludes formation of the hydrogen bond between the backbone carbonyl of Ala 113 and the nitrogen of **12c**, which leaves the Ala 113 backbone carbonyl free to interact with the backbone amide of the N-terminal inhibitor residue of **12a**. This altered role for Ala 113 appears to cause a ~0.5 Å enzyme shift in the region of Ala 113−Phe 114, one of the largest shifts in the active site (Figure 4). In terms of the inhibitor, this interaction, in combination with steric interactions with the DMSO, appears to make the benzyl group favor the alternative conformation seen in the silanediol complex. While the phosphonate **12d** is similar to the silanediol **12a** in that it cannot make a hydrogen bond between (Z) and the Ala 113 carbonyl, its benzyl group remains in the conformation of the phosphonamidate **12c**. This suggests that a combination of factors and not just the absence of a single hydrogen bond results in the alternative benzyl conformation seen in the silanediol **12a**.

The third structural difference between the inhibitors occurs at site Y, where the carbon of the silanediol **12a** is replaced with the oxygen of the phosphonamidate **12c**. With the phosphonamidate, this oxygen atom is 3.3 Å from a water molecule. Such an interaction might be unfavorable with the carbon of the silanediol, which would also make the benzyl residue favor its alternative conformation.

Given that the conformational differences in both enzyme and inhibitor are easily explained by the structural differences between the inhibitors, the implications for future inhibitor design are good. With this work, the possibility of using silicon to create nonhydrolyzable tetrahedral centers for inhibitors and other ligands has now been realized. The structures suggests that silanediols will bind as one would predict; therefore, they can now be used with confidence as structural motifs for drug design.

In summary, we report here the first structure of an organosilane bound to a natural receptor where the silicon interacts with the binding site (*43*). In this case, the ligand binds very similarly to phosphorus-based ligands used in previous studies, with some differences associated with the chemical and structural differences between the respective molecules. The similarities in binding for the phosphorus- and silicon-based inhibitors, both in terms of K_i and modes of binding, might seem surprising based on the neutrality of the silanediol and the anionic nature of the phosphorus groups and their interaction with the cationic zinc ion. Nevertheless, the use of silanediols as rational components for drug design is now on firmer footing.

REFERENCES

1. Leung, D., Abbenante, G., and Fairlie, D. P. (2000) Protease inhibitors: Current status and future prospects, *J. Med. Chem. 43*, 305−341.
2. Barrett, A. G. M. (1991) Reduction of carboxylic acid derivatives to alcohols, ethers, and amines, in *Comprehensive Organic Synthesis* (Trost, B. M., and Fleming, I., Eds.) pp 235−257, Pergamon, New York.
3. Ripka, A. S., and Rich, D. H. (1998) Peptidomimetic design, *Curr. Opin. Chem. Biol. 2*, 441−452.
4. Babine, R. E., and Bender, S. L. (1997) Molecular recognition of protein−ligand complexes: Applications to drug design, *Chem. Rev. 97*, 1359−1472.
5. Borkakoti, N. (2004) Matrix metalloprotease inhibitors: Design from structure, *Biochem. Soc. Trans. 32*, 17−20.
6. Vane, J. R. (1999) The history of inhibitors of angiotensin converting enzyme, *J. Physiol. Pharmacol. 50*, 489−498.
7. Sawa, M. (2003) Phosphonamide-based metalloproteinase inhibitors: A new approach to the development of safer metalloproteinase inhibitors, *Curr. Med. Chem. 2*, 367−378.
8. Clark, I. M., and Parker, A. E. (2003) Metalloproteinases: Their role in arthritis and potential as therapeutic targets, *Expert Opin. Ther. Targets 7*, 19−34.
9. Matthews, B. W., Weaver, L. H., and Kester, W. R. (1974) The conformation of thermolysin, *J. Biol. Chem. 249*, 8030−8044.
10. Hangauer, D. G., Monzingo, A. F., and Matthews, B. W. (1984) An interactive computer graphics study of thermolysin-catalyzed peptide cleavage and inhibition by *N*-carboxymethyl dipeptides, *Biochemistry 23*, 5730−3741.
11. Rich, D. H. (1990) Peptidase inhibitors, in *Comprehensive Medicinal Chemistry* (Hansch, C., Sammes, P. G., and Taylor, J. B., Eds.) pp 391−441, Pergamon, New York.
12. Reiter, L. A., Martinelli, G. J., Reeves, L. A., and Mitchell, P. G. (2000) Difluoroketones as inhibitors of matrix metalloprotease-13, *Bioorg. Med. Chem. Lett. 10*, 1581−1584.
13. Beckett, R. P., Davidson, A. H., Drummond, A. H., Huxley, P., and Whittaker, M. (1996) Recent advances in matrix metalloproteinase inhibitor research, *Drug Discovery Today 1*, 16−25.
14. Chen, C.-A., Sieburth, S. McN., Glekas, A., Hewitt, G. W., Trainor, G. L., Erickson-Viitanen, S., Garber, S. S., Cordova, B., Jeffrey, S., and Klabe, R. M. (2001) Drug design with a new transition state analogue of the hydrated carbonyl: Silicon-based inhibitors of the HIV protease, *Chem. Biol. 8*, 1161−1166.
15. Mutahi, M. w., Nittoli, T., Guo, L., and Sieburth, S. McN. (2002) Silicon-based metalloprotease inhibitors: Synthesis and evaluation of silanol and silanediol peptide analogues as inhibitors of angiotensin-converting enzyme (ACE), *J. Am. Chem. Soc. 124*, 7363−7375.
16. Kim, J., and Sieburth, S. McN. (2004) Silanediol peptidomimetics. Evaluation of four diastereomeric ACE inhibitors, *Bioorg. Med. Chem. Lett. 14*, 2853−2856.
17. Kim, J., Hewitt, G., Carroll, P., and Sieburth, S. McN. (2005) Silanediol inhibitors of angiotensin-converting enzyme (ACE). Synthesis and evaluation of four diastereomers of Phe[Si]Ala dipeptide analogues, *J. Org. Chem. 70*, 5781−5789.
18. Kim, J., Glekas, A., and Sieburth, S. McN. (2002) Silanediol-based inhibitor of thermolysin, *Bioorg. Med. Chem. Lett. 12*, 3625−3627.
19. Kim, J., and Sieburth, S. McN. (2004) A silanediol inhibitor of the metalloprotease thermolysin: Synthesis and comparison with a phosphinic acid inhibitor, *J. Org. Chem. 69*, 3008−3014.
20. Sieburth, S. McN., Nittoli, T., Mutahi, A. M., and Guo, L. (1998) Silanediols: A new class of potent protease inhibitors, *Angew. Chem. Int. Ed., 37*, 812−814.
21. Collinsova, M., and Jiracek, J. (2000) Phosphinic acid compounds in biochemistry, biology, and medicine, *Curr. Med. Chem. 7*, 629−647.
22. Churchill, M. R., Lake, C. H., Chao, S.-H. L., and Beachley, O. T., Jr. (1993) Silicone grease as a precursor to a pseudo crown

ether ligand: Crystal structure of $[K^+]_3[K(Me2SiO)_7^+]$-$[InH(CH_2CMe_3)^{3-}]_4$, *J. Chem. Soc., Chem. Commun.* 1577−1578.
23. Su, K., Tilley, T. D., and Sailor, M. J. (1996) Molecular and polymer precursor routes to manganexe-doped zinc orthosilicate phosphors, *J. Am. Chem. Soc. 118*, 3459−3468.
24. Miller, R. L., Toreki, T., LaPointe, R. E., Wolczanski, P. T., van Duyne, G. D., and Roe, D. C. (1993) Syntheses, carbonylations, and dihydrogen exchange studies of monomeric and dimeric silox ($^tBu_3SiO^-$) hydrides of tantalum: Structure of $[(silox)_2TaH_2]_2$, *J. Am. Chem. Soc. 115*, 5570−5588.
25. Miller, R. L., Lawler, K. A., Bennett, J. L., and Wolczanski, P. T. (1996) Ditungsten siloxide hydrides, $[(silox)_2WHn]_2$ ($n = 1$, 2; silox equals (t)BuSiO), and related complexes, *Inorg. Chem. 35*, 3242−3253.
26. Morgan, B. P., Scholtz, J. M., Ballinger, M. D., Zipkin, I. D., and Bartlett, P. A. (1991) Differential binding-energy: A detailed evaluation of the influence of hydrogen-bonding and hydrophobic groups on the inhibition of thermolysin by phosphorus-containing inhibitors, *J. Am. Chem. Soc. 113*, 297−307.
27. Grobelny, D., Goli, U. B., and Galardy, R. E. (1989) Binding energetics of phosphorus-containing inhibitors of thermolysin, *Biochemistry 28*, 4948−4951.
28. Holden, H. M., Tronrud, D. E., Monzingo, A. F., Weaver, L. H., and Matthews, B. W. (1987) Slow- and fast-binding inhibitors of thermolysin display different modes of binding: Crystallographic analysis of extended phosphonamidate transition-state analogues, *Biochemistry 26*, 8542−8553.
29. Tronrud, D. E., Holden, H. M., and Matthews, B. W. (1987) Structures of two thermolysin−inhibitor complexes that differ by a single hydrogen bond, *Science 235*, 571−574.
30. Hausrath, A. C., and Matthews, B. W. (2002) Thermolysin in the absence of substrate has an open conformation, *Acta Crystallogr., Sect. D: Biol. Crystallogr. 58*, 1002−1007.
31. Leslie, A. G. W. (1992) Recent changes to the MOSFLM package for processing film and image plate data, *Joint CCP4 and ESF-EAMCB Newsletter on Protein Crystallography, Number 26*.
32. Evans, P. R. (1993) Data reduction, *Proceedings of CCP4 Study Weekend, 1993, on Data Collection and Processing* 114−122.
33. Tronrud, D. E. (1997) The TNT refinement package, *Methods Enzymol. 277*, 306−319.
34. Brunger, A. T. (1993) Assessment of phase accuracy by cross validation: the free *R* value. Methods and applications, *Acta Crystallogr., Sect. D: Biol. Crystallogr. 49*, 24−36.
35. Holland, D. R., Tronrud, D. E., Pley, H. W., Flaherty, K. M., Stark, W., Jansonius, J. N., McKay, D. B., and Matthews, B. W. (1992) Structural comparison suggests that thermolysin and related neutral proteases undergo hinge-bending motion during catalysis, *Biochemistry 31*, 11310−11316.
36. Kraulis, P. J. (1991) MOLSCRIPT: A program to produce both detailed and schematic plots of protein structures, *J. Appl. Crystallogr. 24*, 946−950.
37. Merritt, E. A., and Bacon, D. J. (1997). Raster3D: Photorealistic molecular graphics, *Methods Enzymol. 277*, 505−524.
38. For a detailed comparison between crystal structures of a carbinol, silanediol, and phosphinic acid, see ref 15.
39. Matthews, B. W. (1988) Structural basis of the action of thermolysin and related zinc peptidases, *Acc. Chem. Res. 21*, 333−340.
40. Antonczak, S., Monard, G., Lopez, M. R., and Rivail, J. L. (2000) Insights in the peptide hydrolysis mechanism by thermolysin: A theoretical QM/MM study, *J. Mol. Model. 6*, 527−538.
41. Lickiss, P. D. (1995) The synthesis and structure of organosilanols, *Adv. Inorg. Chem. 42*, 147−262.
42. Lickiss, P. D. (2001) Polysilanols, in *The Chemistry of Organic Silicon Compounds* (Rappoport Z., and Apeloig, Y., Ed.) pp 695−744, John Wiley and Sons, New York.
43. The Protein Data Bank has three structures with silicon as part of the bound ligand. Two have trimethylsilyl substitution on substrate analogues, the third is a silane bound to a catalytic antibody: trimethylsilylmaleate bound to fumarase C (PDB ID 1FUQ), Weaver, T., and Banaszak, L. (1996) Crystallographic studies of the catalytic and a second site in fumarase C from *Escherichia coli*, *Biochemistry 35*, 13955−13965; a 2-trimethylsilylethoxy group on a ganglioside analogue bound to the tetanus binding site (PDB ID 1FV2), Fotinou, C., Emsley, P., Black, I., Ando, H., Ishida, H., Kiso, M., Sinha, K. A., Fairweather, N. F., and Isaacs, N. W. (2001) The crystal structure of tetanus toxin Hc fragment complexed with a synthetic GT1b analogue suggests cross-linking between ganglioside receptors and the toxin, *J. Biol. Chem. 276*, 32274−32281; and a phenyldimethylsilyl-substituted hapten bound to its elicited catalytic antibody (PDB ID 1ND0), Zhu, X., Heine, A., Monnat, F., Houk, K. N., Janda, K. D., and Wilson, I. A. (2003) Structural basis for antibody catalysis of a cationic cyclization reaction, *J. Mol. Biol. 329*, 69−83.
44. McDonald, I. K., and Thornton, J. M. (1994) Satisfying hydrogen bonding potential in proteins, *J. Mol. Biol. 238*, 777−793.
45. Zhang, X.-J., and Matthews, B. W. (1995) EdPDB: A multi-functional tool for protein structure analysis, *J. Appl. Crystallogr. 28*, 624−630.

BI051346V